



Flux pinning and flux creep in $\text{La}_{2-x}\text{Sr}_x\text{CuO}_4$ with splayed columnar defects

M. Terasawa ^{a,*}, N. Takezawa ^b, K. Fukushima ^b, T. Mitamura ^a, X. Fan ^a,
H. Tsubakino ^a, T. Kohara ^a, K. Ueda ^a, Y. Awaya ^c, T. Kambara ^c,
M. Matsuda ^c, G. Tatara ^d

^a Himeji Institute of Technology, 2167 Shosha, Himeji 671-22, Japan

^b Toshiba Research and Development Center, 4-1 Ukishima-cho, Kawasaki-ku, Kawasaki 210, Japan

^c The Institute of Physical and Chemical Research (RIKEN), Wako 351-02, Japan

^d Department of Earth and Space Science, Osaka University, Toyonaka, Osaka 560, Japan

Received 12 August 1996; accepted 25 November 1996

Abstract

The effects of columnar defects with splayed configurations on flux pinning and flux creep were investigated experimentally. Parallel columnar defects and splayed columnar defects were introduced into specimens of $\text{La}_{2-x}\text{Sr}_x\text{CuO}_4$ by high-energy heavy-ion irradiation. A large enhancement of the flux pinning and the critical current density J_c due to the splayed columnar defects was observed. At temperature $T < 15$ K and a magnetic field $H = 0.1$ T, the effective pinning potential U_0 of a specimen with splayed columns was larger than that of a specimen with parallel columns. On the other hand, at $15 \text{ K} \leq T \leq 30 \text{ K}$ and $H = 0.1$ T, U_0 of a specimen with splayed columns was smaller than that of a specimen with parallel columns. © 1998 Elsevier Science B.V.

Keywords: $\text{La}_{2-x}\text{Sr}_x\text{CuO}_4$; Critical current density; Flux creep; Heavy-ion irradiation; Columnar defects

1. Introduction

The discovery of high- T_c cuprate superconductors has fuelled the development of the practical application potential of these materials in magnetic fields at 77 K (the boiling point of nitrogen) and in high magnetic fields at low temperatures. Technological and scientific interest has been focused on the properties of the mixed state of high- T_c cuprates. One of the most important requirements for expanding the

applications of high- T_c superconductors is the improvement of the critical current density J_c in high magnetic fields. To achieve this, the enhancement of the magnetic-flux pinning strength by introduction of strong pinning centers into a superconductor is necessary. Numerous attempts have been made to introduce strong pinning centers into cuprate superconductors [1–32]. One of the more promising approaches is the introduction of columnar defects into high- T_c cuprates by high-energy heavy-ion irradiation [1–14]. The introduction of parallel columnar defects has considerably enhanced the pinning strength in high- T_c cuprates [1–11]. One recent de-

* Corresponding author.

velopment is the improvement of flux pinning by a splay (dispersion in the orientation) of columnar defects. Hwa et al. [29] have suggested that splayed columnar defects lead to larger J_c and smaller flux creep rates than parallel columnar defects. The validity of this suggestion has been examined in several experiments [12–14]. However, the effects of columnar defects with splayed configurations on flux pinning and flux creep have not been sufficiently understood. The most suitable configuration of splayed columnar defects has not yet been identified. To determine this optimal configuration, it is necessary to investigate in detail the non-trivial effects of splayed columnar defects on flux pinning. A sufficient understanding of these effects will permit the design of the optimal column configuration and lead to the further enhancement of J_c and further reduction of flux creep in the presence of a magnetic field.

We reported in a previous work that, by 3.5 GeV Xe ion irradiation, parallel columnar defects with a diameter of about 5 nm were formed and strong effects on the flux pinning, increasing J_c , were observed in $\text{La}_{2-x}\text{Sr}_x\text{CuO}_4$ [10]. The purpose of the present study is to investigate the effect of columnar defects with a splayed configuration on the flux pinning and the flux creep in $\text{La}_{2-x}\text{Sr}_x\text{CuO}_4$. For this purpose, we prepared three specimens of $\text{La}_{1.85}\text{Sr}_{0.15}\text{CuO}_4$; a specimen with splayed columnar defects, a specimen with parallel columnar defects, and an unirradiated specimen. Splayed columnar defects and parallel columnar defects were introduced into specimens of $\text{La}_{1.85}\text{Sr}_{0.15}\text{CuO}_4$ by high-energy heavy-ion irradiation. We measured the magnetic hysteresis and the magnetic relaxation for the three specimens with a superconducting quantum interference device (SQUID) magnetometer. J_c was estimated from the magnetic hysteresis data using the Bean critical state model [33,34]. From the results of the magnetic relaxation, we estimated the effective pinning potential U_0 by using the conventional flux-creep relation [35,36].

In Section 2, the experimental procedure is outlined. The results of experiments on the magnetic hysteresis, the dependence of J_c on the magnetic field, the magnetic relaxation and the dependence of U_0 on T in irradiated specimens of $\text{La}_{1.85}\text{Sr}_{0.15}\text{CuO}_4$ are presented in Section 3. Finally, in Section 4 the study is summarized.

2. Experiments and analysis

Polycrystalline specimens of $\text{La}_{1.85}\text{Sr}_{0.15}\text{CuO}_4$ were prepared from CuO , La_2O_3 and SrO_3 powders by a conventional ceramic procedure [10]. This specimen had a density of 5.9 g/cm^3 (0.83 theoretical density). Experiments were performed on three specimens of $\text{La}_{1.85}\text{Sr}_{0.15}\text{CuO}_4$; an unirradiated specimen, a specimen with parallel columnar defects, and a specimen with splayed columnar defects. The dimensions of these specimens were $3.05 \times 4.63 \times 0.42 \text{ mm}^3$, $2.46 \times 2.63 \times 0.11 \text{ mm}^3$, and $2.36 \times 2.60 \times 0.11 \text{ mm}^3$, respectively. Columnar defects were produced in specimens of $\text{La}_{1.85}\text{Sr}_{0.15}\text{CuO}_4$ at room temperature by irradiation of 3.5 GeV Xe^{31+} ions, which had a range of 0.19 nm in the specimen according to TRIM91 calculation, indicating that the ions could penetrate through the specimen. Parallel columns were introduced by the ion beam directed parallel to the shortest dimension (the z -axis) of a specimen. Splayed columns were introduced by the ion beam directed at five angles of 0° , $+5^\circ$, -5° , $+10^\circ$ and -10° from the z -axis. In all irradiated specimens, total fluence is $\phi t = 3 \times 10^{11} \text{ ions/cm}^2$, which is equivalent to an area density of vortices at a magnetic field of $B_{\phi t} \cong 6.2 \text{ T}$. Resistivity and AC magnetic susceptibility of all specimens were measured. Critical temperature T_c was about 36 K, in the irradiated specimen as well as the unirradiated specimen. Magnetic measurements were carried out in a Quantum Design SQUID magnetometer with a scan length of 3 cm, which gives a magnetic field variation less than 0.05%. The applied magnetic field H was parallel to the z -axis of the specimen in all measurements. Magnetization hysteresis loops were measured at $T = 5, 20$ and 30 K , respectively, using the following procedure. Initially, each specimen was cooled from room temperature to the selected temperature in zero field to obtain an initial superconducting state with no trapped magnetic flux. H was then increased from 0 to 5 T, and decreased from 5 to -5 T and increased from -5 to 5 T in small steps. The magnetization M as a function of H was recorded at each step. The data of $M(H)$ were corrected for demagnetizing factor. The demagnetizing factor for H parallel to the z -axis of the specimen, D , was calculated by using the formula for oblate spheroids [37]. In cgs units, we obtained

$D = 11$ for the unirradiated specimen, $D = 12$ for the specimen with parallel columnar defects, and $D = 12$ for the specimen with splayed columnar defects. Corrections for demagnetization are given by transforming H into the effective magnetic field $H_{\text{eff}} = H - DM$. From the difference between the magnetization in the decreasing field and that in the increasing field, ΔM , we calculated J_c flowing in the ab -plane using the Bean critical state model [33,34]. For a rectangular parallelepiped specimen with sides $a_1 \times a_2$ ($a_2 > a_1$), J_c is expressed as

$$J_c = \frac{20\Delta M}{a_1(1 - a_1/3a_2)}, \quad (1)$$

where J_c is in A/cm², ΔM is in emu/cm³, and a_1 and a_2 are in cm [34]. The measurement of magnetic relaxation was carried out at $T = 5, 10, 15, 20, 25$ and 30 K, respectively, using the following procedure. The specimen was cooled from room temperature to the desired temperature in zero field. H was then raised up to 0.1 T and maintained at this value during the measurements. M was recorded as a function of time at 100 s intervals over a period of 10 000 s. From the results of the decay of M with time, we estimated U_0 . If we use the conventional flux-creep relation

$$M(t) = M_0 \left(1 - \frac{kT}{U_0} \ln \left(\frac{t}{t_0} + 1 \right) \right), \quad (2)$$

where M_0 is the initial magnetization, k is the Boltzmann constant, and t_0 is an arbitrary reference time [35,36], U_0 is obtained as

$$U_0 = kT \left(\frac{dM(t)}{M_0 d \ln(t)} \right)^{-1}. \quad (3)$$

At present, because it is not clear whether the above effective U_0 indicates the true pinning potential, U_p [38], we use U_0 as an effective pinning potential only to examine and compare the flux creep rates in the three specimens.

3. Results and discussion

3.1. Magnetic hysteresis and the critical current density

Fig. 1a–c shows M as a function of H_{eff} at $T = 5, 20$ and 30 K, respectively; for the specimen

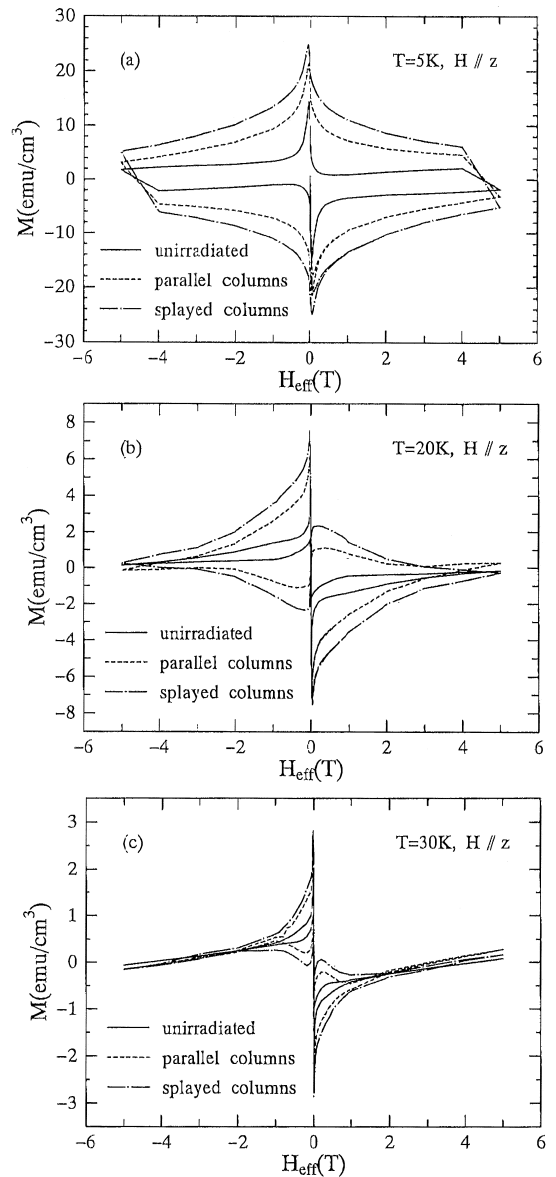


Fig. 1. The magnetization M as a function of the effective field H_{eff} for the unirradiated specimen, the specimen with parallel columnar defects, and the specimen with splayed columnar defects. (a), (b) and (c) correspond to the temperatures $T = 5, 20$ and 30 K, respectively.

with splayed columnar defect, the specimen with parallel columnar defects, and the unirradiated specimen. At $T = 5$ K (Fig. 1a), ΔM is the largest for the specimen with splayed columns up to $H_{\text{eff}} = 4$ T,

and is much larger than for the unirradiated specimen. ΔM for the specimen with parallel columns is smaller than for the specimen with splayed columns, and is much larger than for the unirradiated specimen. At low fields, as the magnitude of H_{eff} increases, ΔM for the specimen with splayed columns decreases at a slower rate than in the case of the other two specimens. Behavior similar to that at 5 K (Fig. 1a) also appears at 20 K (Fig. 1b) and 30 K (Fig. 1c). These results suggest a large enhancement of the flux pinning and J_c due to the splayed configuration of columnar defects.

In Fig. 2a–c, the H_{eff} dependence of J_c for the three specimens is plotted at $T = 5, 20$ and 30 K, respectively. As seen in Fig. 2a, at $T = 5$ K the specimen with splayed columnar defects has the largest J_c up to $H_{\text{eff}} = 4$ T. J_c of the specimen with parallel columns is much larger than that of the unirradiated specimen, while J_c of the specimen with splayed columns is larger than that of the specimen with parallel columns. As H_{eff} increases from 0 to 1 T, J_c for the unirradiated specimen decreases rapidly. At high fields ($1 \text{ T} < H_{\text{eff}} < 4 \text{ T}$), J_c of the unirradiated specimen remains nearly constant. The specimen with splayed pins, however, shows a slower decrease of J_c with increasing H_{eff} than the other two specimens. Thus the enhancement of J_c by splayed pins is the largest in the field range between 0.5 T and 1 T, and decreases slowly with increasing H_{eff} from 1 to 4 T. J_c of the specimen with splayed pins is about twice as large as that of the specimen with parallel pins in the field range between 0.5 T and 1 T.

At $T = 20$ K (Fig. 2b), as in the case of $T = 5$ K, the specimen with splayed columns has the largest value of J_c , and this value is larger than that of the specimen with parallel columns. J_c of the specimen with parallel columns is much larger than that of the unirradiated specimen as in the case of $T = 5$ K. For the unirradiated specimen, as H_{eff} increases, J_c decreases rapidly at low fields ($0 \text{ T} < H_{\text{eff}} < 0.1 \text{ T}$), becomes nearly constant in the field range from 0.1 to 2 T, and decreases gradually at high fields ($2 \text{ T} < H_{\text{eff}} < 4 \text{ T}$). J_c of the specimen with splayed pins, however, falls slowly relative to the other two specimens as H_{eff} increases up to 4 T. As a result the enhancement of J_c by splayed pins is the largest at $H_{\text{eff}} \approx 0.4$ T, and decreases slowly with increasing

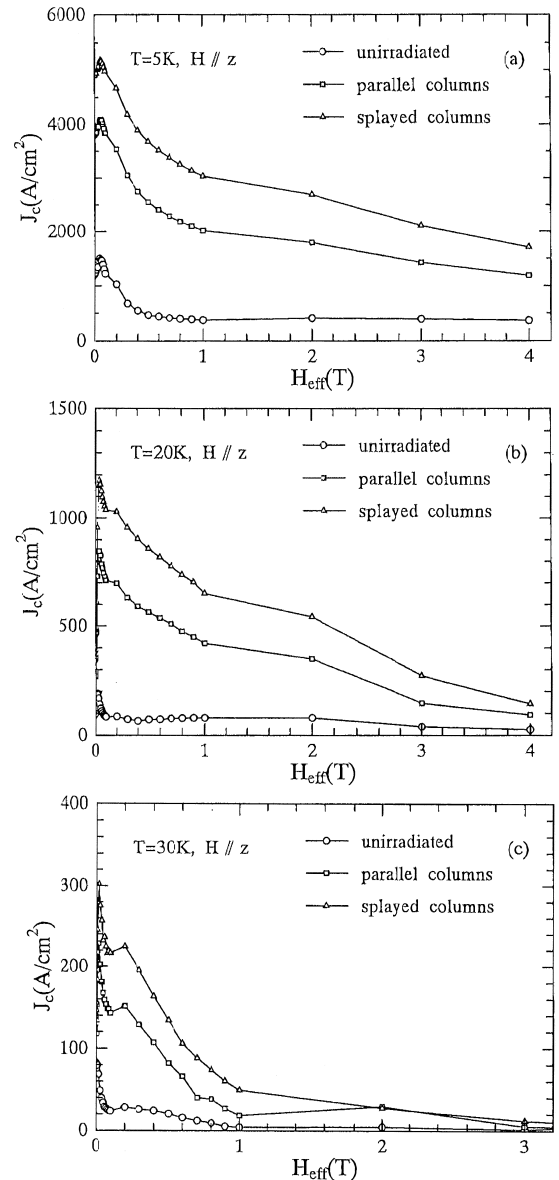


Fig. 2. The critical current density J_c as a function of the effective field H_{eff} for the unirradiated specimen, the specimen with parallel columnar defects, and the specimen with splayed columnar defects. (a), (b) and (c) correspond to the temperatures $T = 5, 20$ and 30 K, respectively.

H_{eff} from 0.1 to 4 T. J_c of the specimen with splayed pins is about twice as large as that of the specimen with parallel pins at $H_{\text{eff}} \approx 0.4$ T.

In the case of $T = 30$ K (Fig. 2c), as in the cases of $T = 5$ and 20 K, J_c of the specimen with splayed

columnar defects is the largest, and is larger than J_c of the specimen with parallel columnar defects. J_c of the specimen with parallel columnar defects is much larger than that of the unirradiated specimen. For the unirradiated specimen, J_c falls off extremely rapidly when H_{eff} is increased from 0 to 0.1 T, becomes nearly constant between 0.1 and 0.2 T, decreases slowly between 0.2 and 1 T, and becomes almost zero at high fields ($1 \text{ T} < H_{\text{eff}}$). J_c values of the specimens with splayed pins and with parallel pins fall off extremely rapidly when H_{eff} is increased from 0 to 0.1 T, become nearly constant between 0.1 and 0.2 T, and decrease slowly between 0.2 and 1 T. The enhancement of J_c by splayed pins is the largest at $H_{\text{eff}} \approx 1 \text{ T}$. J_c of the specimen with splayed pins is about twice as large as that of the specimen with parallel pins at $H_{\text{eff}} \approx 1 \text{ T}$. These results demonstrate that splayed columnar defects enhance flux pinning and J_c to values that are significantly greater than that for parallel columnar defects. At all measured temperatures ($T = 5, 20$ and 30 K) the enhancement of J_c by splayed columns is the largest at low fields, and tends to decrease as H_{eff} increases. This feature can be qualitatively explained by the theory of Hwa et al. [29]. In their theory flux lines are forced to be entangled, since flux lines pass through the crossed columns. In the entangled vortex state the most weakly pinned flux lines are not depinned without cutting their neighbor flux lines pinned more strongly. They are held by interactions with their neighbors pinned more strongly if the flux cutting barrier is larger than the energy corresponding to the temperature. Flux cutting barriers, hence, reduce flux creep and increase J_c . Field dependence of the flux cutting barriers will affect the enhancement strength of J_c by splayed columns. Since the flux cutting barrier increases with decreasing the flux line density [39], the enhancement strength of J_c by splayed columns is expected to decrease with increasing H_{eff} .

3.2. Magnetic relaxation and effective pinning potential

In Fig. 3a–f, the dependence of M normalized against M_0 on time t is plotted for $H = 0.1 \text{ T}$ at $T = 5, 10, 15, 20, 25$ and 30 K , respectively, for the three specimens. The magnetization was observed to be linearly dependent on the logarithm of time at all

measured temperatures for all specimens. At $T = 5 \text{ K}$ (Fig. 3a), the decay of M/M_0 with time for the specimen with splayed pins is the slowest, and is much slower than that of the unirradiated specimen. The decay of M/M_0 with time for the specimen with parallel pins is somewhat faster than that for the specimen with splayed pins, though the difference is very little, and is much slower than that of the unirradiated specimen. In the case of $T = 10 \text{ K}$ (Fig. 3b), the decay of M/M_0 with time for the specimen with splayed pins is the slowest, and is somewhat slower than that of the unirradiated specimen. The decay of M/M_0 with time for the specimen with parallel pins is slightly faster than that of the specimen with splayed pins, and is slightly slower than that of the unirradiated specimen.

On the other hand, at $T = 15 \text{ K}$ (Fig. 3c) and 20 K (Fig. 3d), the decays of M/M_0 with time for both specimens with splayed and parallel pins are almost same, and are much faster than the decay of M/M_0 with time for the unirradiated specimen. At $T = 25 \text{ K}$ (Fig. 3e) and 30 K (Fig. 3f), the decay of M/M_0 with time for the specimen with parallel pins is slower than that for the specimen with splayed pins, and the decays for both specimens are much faster than the decay of M/M_0 with time for the unirradiated specimen. In low fields, the splay configuration of columnar defects appears to suppress the flux creep at low temperatures, while promoting the flux creep at high temperatures.

Fig. 4 shows the dependence of U_0 on T at $H = 0.1 \text{ T}$ for the three specimens. In the temperature range from 5 K to 30 K , U_0 of all specimens increases as T increases. This type of behavior has been observed in other high- T_c cuprates [38,40]. At the lowest temperature ($T = 5 \text{ K}$), the specimen with a splay of columnar defects has the largest U_0 ($= 0.022 \text{ eV}$). This U_0 is about twice as large as that of the unirradiated specimen ($= 0.012 \text{ eV}$). U_0 of the specimen with parallel columnar defects ($= 0.020 \text{ eV}$) is smaller than that of the specimen with splayed columnar defects. At $T = 10 \text{ K}$, U_0 of the specimen with a splay of columnar defects ($= 0.051 \text{ eV}$) is largest. U_0 of the specimen with parallel columnar defects is 0.048 eV , and that of the unirradiated specimen is 0.045 eV . On the other hand, at $T \geq 15 \text{ K}$, the specimen with a splay of columnar defects has the smallest U_0 . In the case of $T = 15 \text{ K}$, U_0 values

are 0.074 and 0.076 eV, respectively, for the specimens with splayed and parallel columns, and they are much smaller than U_0 for the unirradiated specimen ($= 0.11$ eV). At $T = 20$ K, U_0 values are 0.100 eV and 0.104 eV, respectively, for the specimens with splayed and parallel columns, and they are

smaller than U_0 for the unirradiated specimen ($= 0.174$ eV). In the case of $T = 25$ and 30 K, U_0 for the specimen with splayed columns is about half of that for the unirradiated specimen. U_0 of the specimen with parallel columns is larger than that of the specimen with splayed columns. These results

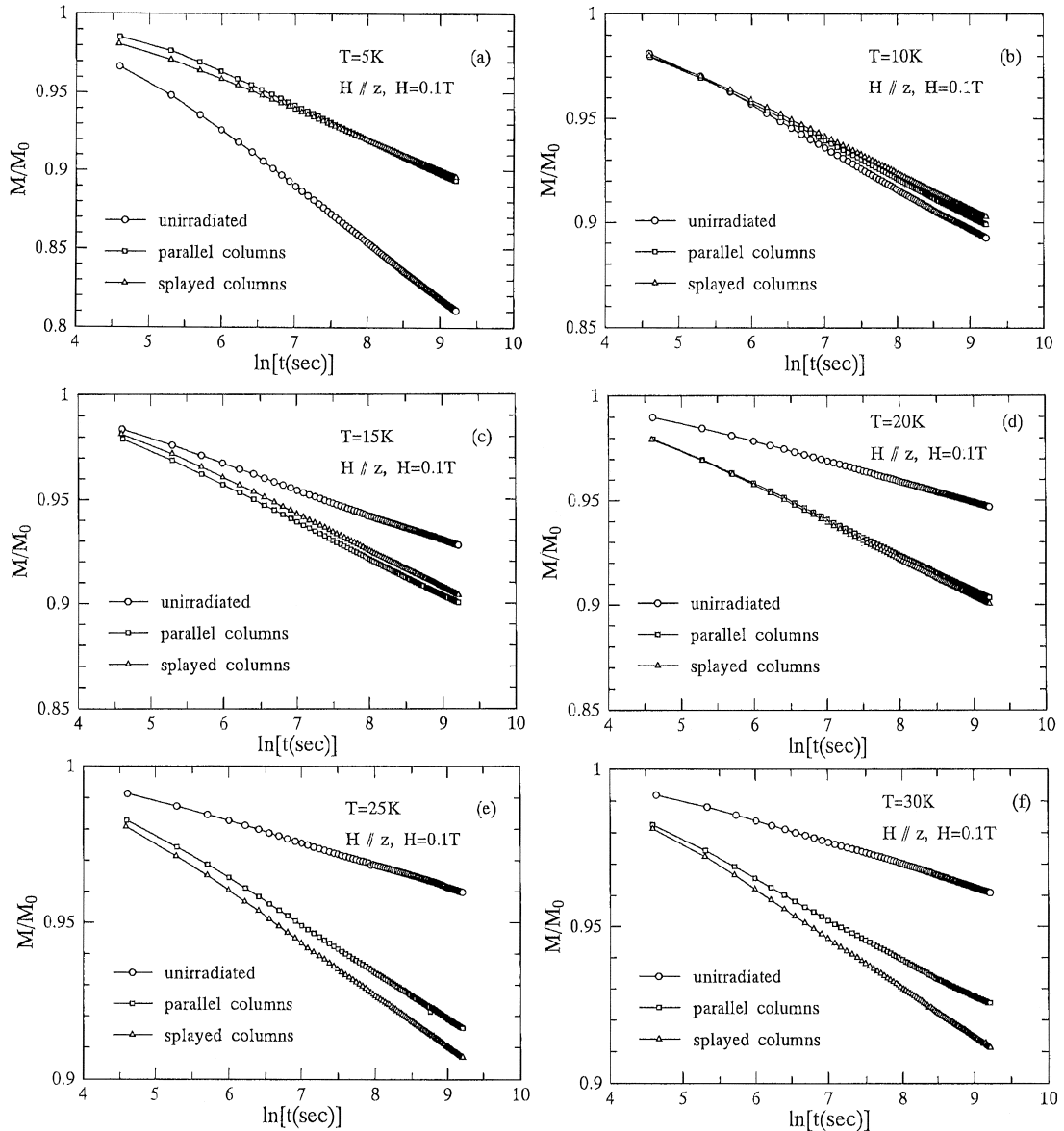


Fig. 3. The magnetization M normalized against the initial magnetization M_0 as a function of time t for the applied field $H = 0.1$ T for the unirradiated specimen, the specimen with parallel columnar defects, and the specimen with splayed columnar defects. (a), (b), (c), (d), (e) and (f) correspond to the temperatures $T = 5, 10, 15, 20, 25$ and 30 K, respectively.

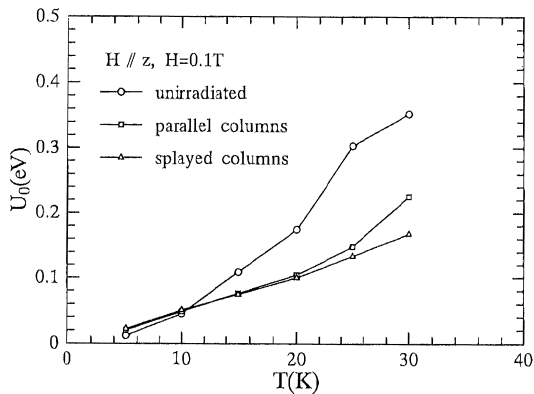


Fig. 4. The effective pinning potential U_0 as a function of temperature T for the applied field $H = 0.1$ T for the unirradiated specimen, the specimen with parallel columnar defects, and the specimen with splayed columnar defects.

indicate that, for $H = 0.1$ T, splayed columnar defects enhance U_0 to values well above those for the other two specimens at low temperatures, and reduce U_0 to values well below those for the other two specimens at high temperatures.

It appears that, at $H = 0.1$ T, there is a cross-over from suppression to promotion of the flux creep by the splay configuration of columnar defects with increasing T . Although Hwa et al. [29] did not predict how splay columns affect temperature dependence of flux creep rates, we tried to interpret our results qualitatively in the light of their theory. In the theory of Hwa et al. there are two main mechanisms which cause a larger reduction of flux creep for splayed columnar defects than for parallel columnar defects. First, the flux line localization on the splayed columns forces flux line entanglement, so that flux cutting barriers reduce flux creep. Second, due to misalignments of columns, splayed columns reduce the vortex transport by the variable-range hopping at low currents more largely than parallel columns. In other words, splayed columns reduce the variable-range hopping since the vortex superkink-pair excitations [41–43], which dominate flux motion, will occur among columns with similar tilts. Flux creep is, hence, suppressed at low currents. Furthermore, the intersections of splayed columns can pin the vortex kinks sliding along the column, and impede the flux depinning from the column, and thus reduce flux creep. However, we must note that the intersec-

tions of splayed columns can also promote flux creep. The intersections can stimulate the vortex kinks nucleation, and make the flux motion between neighbor columns easier, and cause flux lines to form zigzag lines. Then, the zigzag excitations are expected to promote flux creep. As a result of the competition of these mechanisms, splayed columns suppress or promote flux creep in comparison with parallel columns. In our case, at $H = 0.1$ T, a cross-over of dominant mechanism of flux creep by splayed columns with increasing T is seen. The cause of such a cross-over is not clear. To clarify this cause, further investigations, both experimental and theoretical, may be required into the effect of splayed columns on flux pinning and flux creep.

4. Summary

We have investigated the effects of splayed columnar defects on flux pinning and flux creep in specimens of $\text{La}_{1.85}\text{Sr}_{0.15}\text{CuO}_4$. The introduction of parallel columnar defects and splayed columnar defects into specimens of $\text{La}_{1.85}\text{Sr}_{0.15}\text{CuO}_4$ was performed by high-energy heavy-ion irradiation. The magnetic hysteresis and the magnetic relaxation for these specimens were measured with a SQUID magnetometer. We used the Bean model to obtain J_c from the hysteresis of the magnetization. Using the conventional flux-creep relation, we also evaluated U_0 from the magnetic relaxation data. Our results demonstrate a large enhancement in flux pinning and J_c due to the splayed configuration of columnar defects. The flux pinning and J_c for the specimen with splayed columnar defects were significantly greater than those for the unirradiated specimen and the specimen with parallel columnar defects. With regard to the magnetic relaxation, M was seen to have a logarithmic time dependence at all measured temperatures for all specimens. For $H = 0.1$ T, the decay of M/M_0 with time for the specimen with splayed columns was found to be slowest at low temperatures and fastest at high temperatures. For $H = 0.1$ T, splayed columnar defects were seen to enhance U_0 to values well above those for the unirradiated specimen and the specimen with parallel columnar defects at low temperatures ($T < 15$ K),

and reduce U_0 to values well below those for the unirradiated specimen and the specimen with parallel columnar defects at high temperatures ($15 \text{ K} \leq T \leq 30 \text{ K}$).

References

- [1] V. Hardy, D. Groult, M. Hervieu, J. Provost, B. Raveau, S. Bouffard, *Nucl. Instrum. Meth. B* 54 (1991) 472.
- [2] L. Civale, A.D. Marwick, T.K. Worthington, M.A. Kirk, J.R. Thompson, L. Krusin-Elbaum, Y. Sun, J.R. Clem, F. Holtzberg, *Phys. Rev. Lett.* 67 (1991) 648.
- [3] M. Konczykowski, F. Rullier-Albenque, E.R. Yacoby, A. Shaulov, Y. Yeshurun, P. Lejay, *Phys. Rev. B* 44 (1991) 7167.
- [4] M. Konczykowski, V.M. Vinokur, F. Rullier-Albenque, Y. Yeshurun, F. Holtzberg, *Phys. Rev. B* 47 (1993) 5531.
- [5] L. Klein, E.R. Yacoby, Y. Wolfus, Y. Yeshurun, L. Burlachkov, D.Ya. Shapiro, M. Konczykowski, F. Holtzberg, *Phys. Rev. B* 47 (1993) 12349.
- [6] W. Gerhauser, G. Ries, H.W. Neumüller, W. Schmidt, O. Eibl, G. Saemann-Ischenko, S. Klaumünzer, *Phys. Rev. Lett.* 68 (1992) 879.
- [7] J.R. Thompson, Y.R. Sun, H.R. Kerchner, D.K. Christen, B.C. Sales, B.G. Chakoumakos, A.D. Marwick, L. Civale, J.O. Thomson, *Appl. Phys. Lett.* 60 (1992) 2306.
- [8] R.C. Budhani, M. Suenaga, S.H. Liou, *Phys. Rev. Lett.* 69 (1992) 3816.
- [9] J.E. Tkaczyk, J.A. DeLuca, P.L. Karas, P.J. Bednarczyk, D.K. Christen, C.E. Klabunde, H.R. Kerchner, *Appl. Phys. Lett.* 62 (1993) 3031.
- [10] M. Terasawa, T. Mitamura, T. Kohara, K. Ueda, H. Tsubakino, A. Yamamoto, Y. Awaya, T. Kambara, Y. Kanai, M. Oura, Y. Nakai, *Physica C* 235–240 (1994) 2805.
- [11] Th. Becker, H. Theuss, Th. Schuster, H. Kronmüller, M. Kraus, G. Saemann-Ischenko, *Physica C* 245 (1995) 273.
- [12] L. Krusin-Elbaum, J.R. Thompson, R. Wheeler, A.D. Marwick, C. Li, S. Patel, D.T. Shaw, P. Lisowski, J. Ullmann, *Appl. Phys. Lett.* 64 (1994) 3331.
- [13] L. Civale, L. Krusin-Elbaum, J.R. Thompson, R. Wheeler, A.D. Marwick, M.A. Kirk, Y.R. Sun, F. Holtzberg, C. Feild, *Phys. Rev. B* 50 (1994) 4102.
- [14] Th. Schuster, H. Kuhn, M.V. Indenbom, M. Leghissa, M. Kraus, M. Konczykowski, *Phys. Rev. B* 51 (1995) 16358.
- [15] M. Murakami, M. Morita, K. Doi, K. Miyamoto, *Jpn. J. Appl. Phys.* 28 (1989) 1189.
- [16] M. Murakami, S. Gotoh, N. Koshizuka, S. Tanaka, T. Matsushita, S. Kambe, K. Kitazawa, *Cryogenics* 30 (1990) 390.
- [17] S. Jin, T.H. Tiefel, S. Nakahara, J.E. Graebner, H.M. O'Bryan, R.A. Fastnacht, G.W. Kammlott, *Appl. Phys.* 56 (1990) 1287.
- [18] K. Watanabe, T. Matsushita, N. Kobayashi, H. Kawabe, E. Aoyagi, K. Hiraga, H. Yamane, H. Kurosawa, T. Hirai, Y. Muto, *Appl. Phys. Lett.* 56 (1990) 1490.
- [19] Y.Q. Li, J. Zhao, C.S. Chern, P. Lu, T.R. Chien, B. Gallois, P. Norris, B. Kear, F. Cosandey, *Appl. Phys. Lett.* 60 (1992) 2430.
- [20] D. Shi, M.S. Boley, U. Welp, J.G. Chen, Y. Liao, *Phys. Rev. B* 40 (1989) 5255.
- [21] F.M. Sauerzopf, H.P. Wiesinger, W. Kritscha, H.W. Weber, G.W. Crabtree, J.Z. Liu, *Phys. Rev. B* 43 (1991) 3091.
- [22] W. Kritscha, F.M. Sauerzopf, H.W. Weber, G.W. Crabtree, Y.C. Chang, P.Z. Jiang, *Europhys. Lett.* 12 (1990) 179.
- [23] K. Shiraishi, T. Kato, J. Kuniya, *Jpn. Appl. Phys.* 28 (1989) L807.
- [24] T. Terai, T. Masegi, K. Kusagaya, Y. Takahashi, K. Kishio, N. Motohira, K. Nakatani, *Physica C* 185–189 (1991) 2383.
- [25] L. Civale, A.D. Marwick, M.W. McElfresh, T.K. Worthington, A.P. Malozemoff, F.H. Holtzberg, J.R. Thompson, M.A. Kirk, *Phys. Rev. Lett.* 65 (1990) 1164.
- [26] L.W. Lombardo, D.B. Mitzi, A. Kapitulnik, A. Leone, *Phys. Rev. B* 46 (1992) 5615.
- [27] K. Fukushima, H. Adachi, *Physica C* 207 (1993) 119.
- [28] K. Fukushima, *Physica C* 212 (1993) 407.
- [29] T. Hwa, P. Le Doussal, D.R. Nelson, V.M. Vinokur, *Phys. Rev. Lett.* 71 (1993) 3545.
- [30] P. Le Doussal, D.R. Nelson, *Physica C* 232 (1994) 69.
- [31] N. Takezawa, K. Fukushima, *Physica C* 228 (1994) 149.
- [32] N. Takezawa, K. Fukushima, in: K. Yamafuji, T. Morishita (Eds.), *Advances in Superconductivity VII*, Springer, Tokyo, 1995, p. 485.
- [33] C.P. Bean, *Rev. Mod. Phys.* 36 (1964) 31.
- [34] A.M. Campbell, J.E. Evetts, *Adv. Phys.* 21 (1972) 199.
- [35] P.W. Anderson, Y.B. Kim, *Rev. Mod. Phys.* 36 (1964) 39.
- [36] M.R. Beasley, R. Labusch, W.W. Webb, *Phys. Rev.* 181 (1969) 632.
- [37] J.A. Osborn, *Phys. Rev.* 67 (1945) 351.
- [38] Y. Xu, M. Suenaga, A.R. Moodenbaugh, D.O. Welch, *Phys. Rev. B* 40 (1989) 10882.
- [39] C. Carraro, D.S. Fisher, *Phys. Rev. B* 51 (1995) 534.
- [40] C.W. Hagen, R. Griessen, *Phys. Rev. Lett.* 62 (1989) 2857.
- [41] E.H. Brandt, *Europhys. Lett.* 18 (1992) 635.
- [42] E.H. Brandt, *Phys. Rev. Lett.* 69 (1992) 1105.
- [43] D.R. Nelson, V.M. Vinokur, *Phys. Rev. Lett.* 68 (1992) 2398.